Measurement of the Momentum Flux in an Ion Beam

IEPC-2011-232

Presented at the 32nd International Electric Propulsion Conference,
Wiesbaden • Germany
September 11 – 15, 2011

Alexander Spethmann[1] , Thomas Trottenberg[2] , and Holger Kersten[3]
Institute of Experimental and Applied Physics, University of Kiel, 24098 Kiel, Germany

Abstract: This paper reports on our first realization of a novel force measuring diagnostic for ion beams and plasmas with spatial resolution. First measurements have been performed in the beam of an electron cyclotron resonance ion source. Radial measurements allow to record the beam profile of the source. It is found that axial measurements of forces in combination with measurements of electric currents are well described by taking into account charge-exchange collisions. Both radial and axial measurements are in good agreement with a simple beam model based on the superposition of diverging beamlets.

Nomenclature

A	= size of the target area
W_i	= ion energy
$b(r, z, \vartheta)$	= normalized beamlet profile
r	= radial distance from axis of a single beamlet
z	= distance from the ion source
ϑ	= divergence half-angle of a beamlet
$B(z, \vartheta)$	= normalized beam profile
m_i	= ion mass
λ_{cx}	= mean free path for charge-exchange collisions
F_i, F_n, F_{i+n}, F_0	= ion, neutral, total and initial (at the grid) force acting on the target
$\Gamma_i, \Gamma_n, \Gamma_{i+n}, \Gamma_0$	= ion, neutral, total and initial (at the grid) beam flux
R	= radius of the ion source grids
U_{anode}	= anode voltage of the ion source
U_{grid}	= outer (accelerator) grid potential of the ion source
I_0	= ion beam current at the grids
U_{pp1}, U_{pp2}	= plasma potential in the ion source and in the target vacuum chamber (measured relative to the walls)
n_n	= background gas density

[1]PhD student, Plasma Technology, spethmann@physik.uni-kiel.de
[2]Research Associate, Plasma Technology, trottenberg@physik.uni-kiel.de
[3]Professor, Plasma Technology, kersten@physik.uni-kiel.de.

I. Introduction

Measurements of low thrusts of ion engines are a challenge, however, they are necessary for development and testing of ion thrusters for space missions. A calculation of the thrust from the beam current, which is easier to measure, is not a solution, because part of the ion beam might have been neutralized by charge-exchange collisions with residual neutral gas in the test chamber. While direct thrust measurements by thrust balances aim to measure the thrust vector, further information about beam composition, beam profile and beam divergence requires spatially resolved measurements in the plume. Therefore, beam diagnostics with spatial resolution are beneficial for development and optimization of propulsion engines.

Several attempts to measure forces of plasma flows with spatial resolution were made recently. They all have in common that momentum fluxes are absorbed by a planar target. Chavers et al. [1] developed a force probe for plasma and neutral particle jets with a target of 5 cm diameter based on a strain gauge, which captures forces in the order of magnitude of 10^{-4} N. The same approach was made for Hall thrusters with forces in the order of Millinewtons and higher [2,3]. Force probes based on pendulum displacements enable measurements of smaller forces in the order of Micronewtons [4,5,6,7,8,9].

In this contribution, we introduce a novel realization of an active force measuring probe. The probe is based on a galvanometer carrying a target and electronics for controlling the current through the coil windings. First measurements with the force probe where performed in an ion beam experiment as a well understood test environment. Additional electrical measurements of the ion beam currents to a small target were performed. The comparison of these corresponding measurements enables to differentiate between charged and neutral particles.

II. Experimental Setup

A. Vertical Ion Beam Experiment

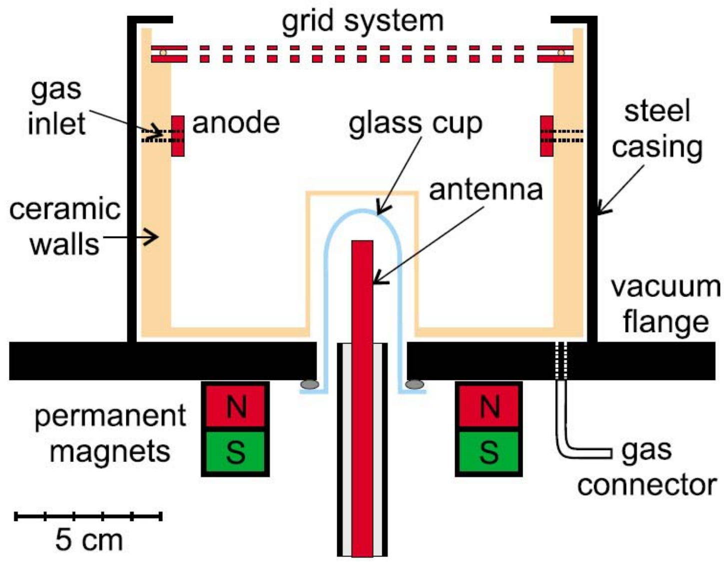

Figure 1. Electron cyclotron resonance ion source.

The ion beam is produced by an industrial broad beam ion source (see Fig. 1) [10]. An argon plasma is generated by microwaves with the help of electron cyclotron resonance. Permanent magnets provide the magnetic field, and an antenna emits approximately 360 W of 2.4 GHz microwaves through a quartz cup into the source chamber. Two plane molybdenum grids with a diameter of 2R = 125 mm and each one with 847 circular 3.2 mm holes extract and accelerate ions from the source plasma. The inner (extraction) grid is floating and the outer (accelerator) grid potential is $U_{grid} = -300$ V throughout this paper. An anode ring in the ceramic source chamber allows to shift the potential of the source plasma by means of the voltage

$U_{anode} = +(0$ - $1000)$ V to corresponding positive potentials $U_{anode} + U_{pp1}$. Measurements with cylindrical Langmuir probes revealed an anode sheath potential drop in the range of $U_{pp1} = +(60 \pm 10)$ V.

The vacuum chamber above the source is basically a vertical stainless steel cylinder with an inner diameter of 30 cm and a height of 40 cm. The pressure in the target chamber is 5×10^{-2} Pa. There are flanges for insertion of radial and axial diagnostics in the walls and the top cover. The ion beam which leaves the source at the bottom is vertically upwards directed and ends after a length of approximately 55 cm at the top cover [11]. The negative potential near the source caused by the accelerator grid decays within a few centimeters due to the screening secondary plasma in the target chamber. The plasma potential U_{pp2} in the target chamber was measured with an emissive probe and is found to be in the range of $U_{pp2} = +(15 \pm 5)$ V, depending on the anode voltage. The potential profiles for a fixed anode voltage show no significant gradient along the vertical axis. The energy of the beam ions $W_i = e(U_{anode} + U_{pp1} - U_{pp2})$ results from the potential drop between source and target plasma.

B. Force Probe

The novel force probe (see Fig. 2) consists basically of a galvanometer. A variable current through the coil windings in the field of permanent magnets causes a torque by means of the Lorentz force. The galvanometer is supplemented by an electrically floating thin planar circular target of 15 mm diameter fixed on a ceramic tube with a counter weight on the opposite side. An optical sensor is detecting the alignment of the ceramic tube. A microcontroller driven algorithm adjusts the pulse width modulated current flowing through the coil windings to keep the ceramic tube in horizontale position. The equilibrium current represents a measure for the exerted force. The galvanometer is protected by a casing of aluminum against heat and currents caused by ion beam and target plasma.

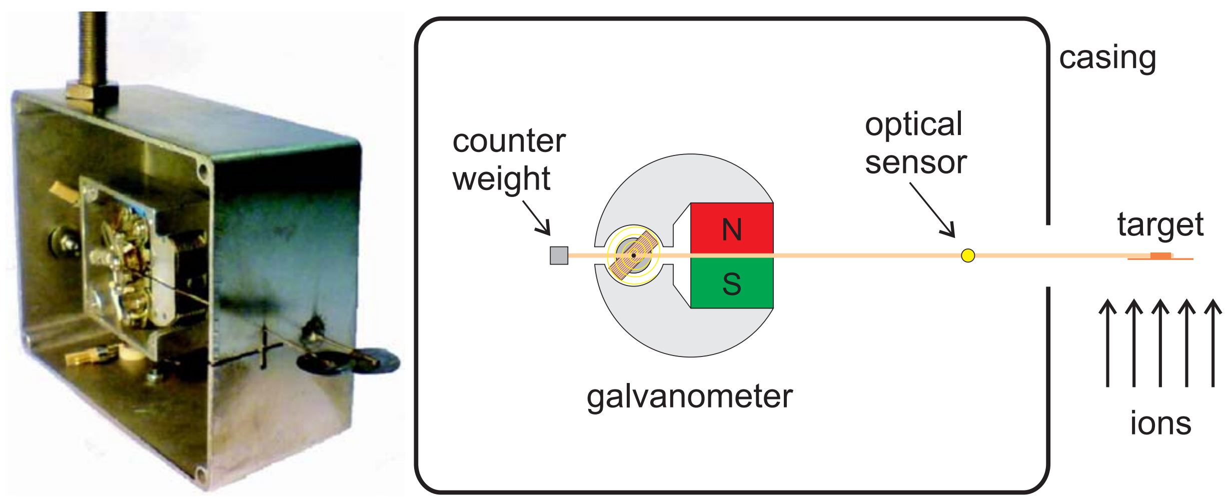

(a) (b)

Figure 2. (a) Photograph and (b) schematic diagram of the force probe. The ceramic tube juts out of the aluminum box and a target consisting of copper is mounted at its end. The second copper target shown in the photograph is optional for electrostatic measurements of currents. The aluminum casing was opened to show the galvanometer.

III. Measurements in ion beam

A. Radial measurements of beam profiles

Radial force measurements are performed to record beam profiles at different energies. Our beam profile model is based on a beam consisting of single beamlets. Accelerated Ar^+ ions from the ion source leave the source through each of the 847 grid holes as beamlets with an assumed Gaussian distribution

$$b(z, r, \vartheta) = \frac{1}{2\,\pi\, z^2\, tan^2\vartheta} \;\exp\left(-\frac{r^2}{2\, z^2\, tan^2\vartheta}\right) \;. \tag{1}$$

The numeric superposition of all beamlets yields the total beam profile of the ion source.

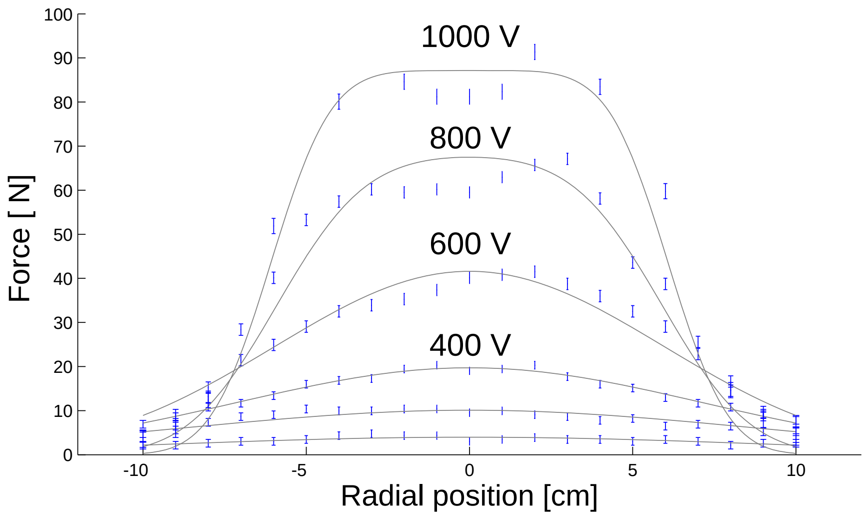

Figure 3. Radial force measurements at different anode voltages.

Radial force measurements (see Fig. 3) were made along the grid-diameter of the ion source in 30 cm height above the grids between -10 and +10 cm around grid centre. Measurement uncertainties are probably caused by an unintended sagging of the probe rod, heating and vibrations, and flow fluctuations of the vacuum pump system. To estimate these uncertainties, some measurements have been done thrice. The maximal differences of the three measurements are plotted as error bars in the plots of axial and radial measurements. The continuous lines display fitted superpositions of Gaussian beamlets described by formula (1). The divergence half-angle ϑ and the initial beam force F_0 are fit parameters. For higher anode voltages (200 V to 1000 V), the beam profiles become more and more box-shaped, according to our model.

B. Axial measurements of charge-exchange collisions

Axial measurements of forces and currents are motivated by an interest in the charge-exchange collisions of Ar^+ and Ar in the target chamber [12,13,14]. The total flux density Γ_{i+n} splits into two components. The ionic component Γ_i can be measured by electrostatic probes, e.g. Faraday cups:

$$\Gamma_i(z) = \Gamma_{i+n}(z) \exp\left(-\frac{z}{\lambda_{cx}}\right) . \quad (2)$$

Measurements of forces do not distinguish between ionic, Γ_i, and neutral components,

$$\Gamma_n(z) = \Gamma_{i+n}(z) \left[1 - \exp\left(-\frac{z}{\lambda_{cx}}\right)\right] . \quad (3)$$

The mean free path for charge-exchange collisions $\lambda_{cx} = 1/(\sigma_{cx} n_n)$ is dependend on the background gas density $n_n = 5 \times 10^{-2}$ Pa. Approximations by Phelps [14] based on measured charge-exchange collisions of ions with energies $E_i > 100$ eV and neutral atoms of the background gas yield a net cross section of approximately $\sigma_{cx} = 5.75 \times 10^{-19}\ (W_i/eV)^{-0.1} m^2$. The resulting mean free path length for beam energies from 260 eV to 460 eV is increasing from 24.9 cm to 26.5 cm. The axial measurements are performed at distances from 14 cm to 48 cm to the ion source.

Beside this height-dependent modification of the beam composition, the beam divergence causes additionally a decreasing total flux density $\Gamma_{i+n}(z)$. With the initial beam density $\Gamma_0 = \Gamma_{i+n}(0)$ at the grids, the vertical beam density becomes

$$\Gamma_{i+n}(z) = B(z,\vartheta)\ \Gamma_0 = \left[1 - \exp\left(\frac{R^2}{2\, z^2\, tan^2\vartheta}\right)\right] \Gamma_0 . \quad (4)$$

The force exerted on the target of the force probe includes both ions and fast neutral atoms, and is modified by the geometrical divergence factor $B(z, \vartheta)$:

$$F_{i+n}(z) = B(z, \vartheta)\, F_0 = B(\vartheta, z) \;\; A\, m_i \left(\frac{2Wi}{m_i} \right)^{\frac{1}{2}} (\Gamma_i + \Gamma_n) \; . \tag{5}$$

In contrast, the measured ion beam currents are additionally modified by charge-exchange collisions:

$$I(z) = B(z, \vartheta)\, I_0 \, \exp\left(-\frac{z}{\lambda_{cx}} \right) \; . \tag{6}$$

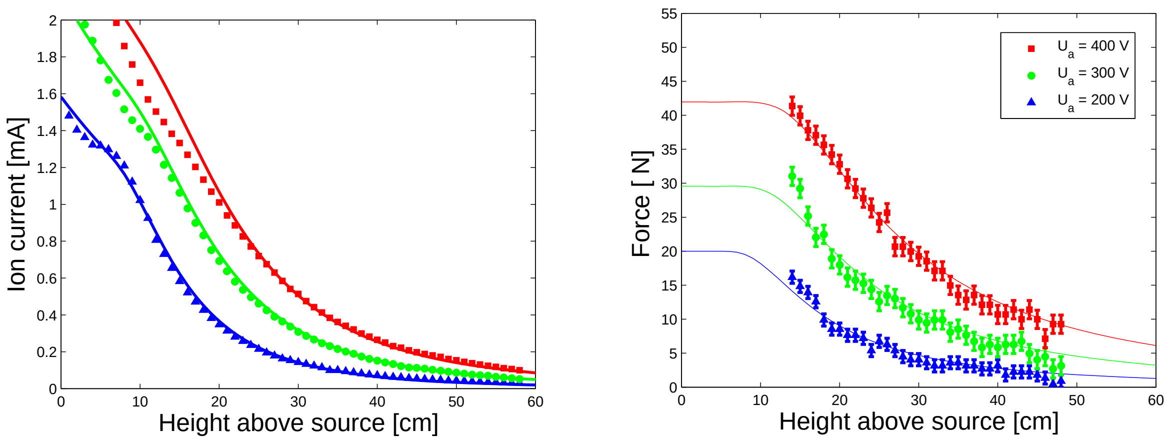

(a) (b)

Figure 4. (a) Measured currents in the beam are fitted considering both divergence and charge-exchange collisions. (b) Measured forces are fitted considering beam divergence only.

Axial force measurements were made at distances from 14 to 48 cm height from the center of the ion source. They were combined with measurements of ion beam currents. First, the measured ion currents (see Fig. 4 a) were fitted with formula (6) (continuous line), where the divergence half-angle ϑ and the ion beam current at the grids I_0 are fit parameters. Measurement points of forces (see Fig. 4 b) were then fitted by formula (5), where the divergence half-angle ϑ is taken from the current fit.

C. Divergence half-angles

The divergence half-angles can be determined by both radial and axial profiles.

Figure 5 shows the divergence half-angles obtained as fit parameters from the radial and axial measurements. Radial measurement points are plotted as blue squares, while those of axial measurements are plotted as green circles. The red line is a linear fit for the radial measurements and indicates the trend of decreasing divergence half-angles for higher beam energies.

IV. Conclusion

Development and testing of ion thrusters require sophisticated beam diagnostics and thrust measurements. Therefore, the described first realization of a force probe with spatial resolution in the Micronewton range can be a useful extension for standard diagnostics. Especially in combination with current measurements, neutral species produced by charge-exchange collisions can be detected, which is of special importance in test chambers.

Acknowledgments

The technical assistance of Volker Rohwer is gratefully acknowledged.

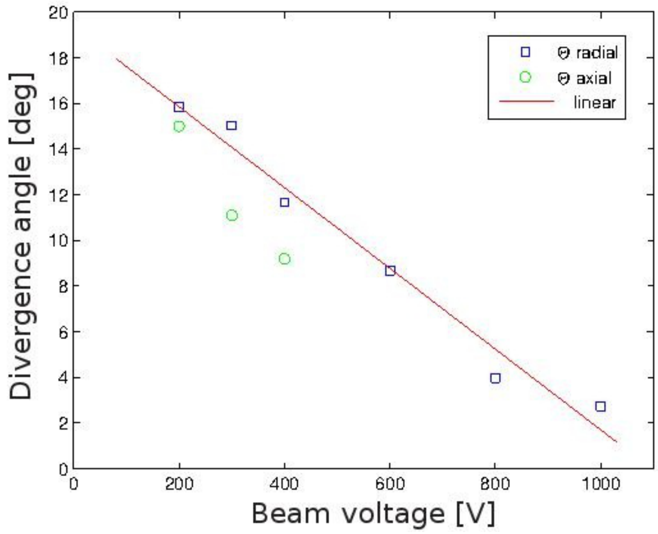

Figure 5. Divergence half-angles of radial and axial measurements. The line is a linear fit for the radial measurements.

References

[1]D. G. Chavers, F. R. Chang-Diaz, "Momentum flux measuring instrument for neutral and charged particle flows," *Review of Scientific Instruments*, 73, 3500-3507, 2002

[2]B. W. Longmier, B. M. Reid, A. D. Gallimore, F. R. Chang-Diaz, J. P. Squire, T. W. Glover, G. Chavers, E. A. Bering III., "Validating a Plasma Momentum Flux Sensor to an Inverted Pendulum Thrust Stand," *Journal of Propulsion and Power*, 25, 746752 , 2009.

[3]R. J. Stephen, K. Rajanna, V. Dhar, K. G. K. Kumar, and S. Nagabushanam, "Thin-Film Strain Gauge Sensors for Ion Thrust Measurement," *IEEE Sensors Journal*, 4, 373377, 2004.

[4]M. D. West, C. Charles, R. W. Boswell, "A high sensitivity momentum flux measuring instrument for plasma thruster exhausts and diffusive plasmas," *Review of Scientific Instruments*, 80, 053509, 2009.

[5]G. Makrinich, A. Fruchtman, "Experimental study of a radial plasma source," *Physics of Plasmas*, 16, 043507, 2009.

[6]K. Kuriki, Y.Y. Kitora, "Momentum transfer to target from laser-produced plasma," *Applied Physics Letters*, 30, 443-446, 2009.

[7]S. Rocca, C. Menon, D. Nicolini, "FEEP micro-thrust balance characterization and testing," *Measurement Science and Technology*, 17, 711, 2006.

[8]D. Packan, J. Bonnet, S. Rocca, "Thrust Measurements with the ONERA Micronewton Balance," *IEPC*, 185, 2009.

[9]P. Gessini, G. M. Sandonato, R. T. Irita, J. A. N. Goncalves, G. Favale e Fernandes, "A pendulum Target Balance for Ion Engine Thrust Measurement," *IEPC*, 149, 2007.

[10]M. Zeuner, F. Scholze, H. Neumann, T. Chasse, G. Otto, D. Roth, A. Hellmich and B. Ocker, "A unique ECR broad beam source for thin film processing," *Surface and Coatings Technology*, Vol. 142-144, 2001, pp. 11-20.

[11]V. Schneider, T. Trottenberg, I. Teliban, H. Kersten "An experiment for the investigation of forces on microparticles in ion beams," *Review of Scientific Instruments*, Vol. 142-144, 2001, pp. 11-20.

[12]T. Trottenberg, V. Schneider, H. Kersten "Measurement of the force on microparticles in a beam of energetic ions and neutral atoms," *Physics of Plasmas*, 17, 103702, 2010

[13]W. Aberth, D. C. Lorentz, "Elastic Differential Scattering of He^+ Ions by Ne and Ar and of Ar^+ Ions by Ar in the 10-600 eV Range," *Physical Review*, 144, 109-115, 1966.

[14]A. V. Phelps, "The application of scattering cross sections to ion flux models in discharge sheats," *Journal of Applied Physics*, Vol. 76, No. 2, 1994, pp. 747-753.